

Experimental study of electron- and ion-beam properties on the BNL electron-beam ion source and comparison with theoretical models

A. Pikin, J. G. Alessi, E. N. Beebe, A. Kponou, and K. Prelec
Brookhaven National Laboratory, Upton, New York 11973

(Presented on 16 September 2005; published online 23 March 2006)

The maximum achievable perveance of the electron beam in the ion trap region and in the electron collector of the BNL Test electron-beam ion source (EBIS) has been measured for different electron-beam currents. These perveances determine the maximum degree of electron-beam retardation in these areas, which limits for the first case the maximum capacity of the ion trap, and for the second case the minimum dissipated power on the electron collector, for a given electron current. The results are compared with the results of optical simulations of the electron beam. In another set of experiments, data on Test EBIS ionization efficiency for different experimental conditions were obtained. These results are presented and compared with calculations based on stepwise ionization assuming 100% ion confinement in the trap. Finally, a series of experimentally measured longitudinal-energy spectra of the extracted ion beam are presented, and will be compared with the calculated energy spread. © 2006 American Institute of Physics.

[DOI: [10.1063/1.2149377](https://doi.org/10.1063/1.2149377)]

I. INTRODUCTION

With high electron current operation (up to 10 A) the BNL Test electron-beam ion source (EBIS) has demonstrated so far a performance that fits the commonly accepted classical phenomenological model of EBIS first proposed by Donets.¹ It was experimentally proved that on the BNL Test EBIS the total extracted ion charge from the trap is proportional to the electron current (for fixed electron energy)² and to the length of ion trap.³

For high current EBIS operation it is very important to predict the confinement time necessary for producing ions of the required charge state as accurately as possible, because it determines the electron-beam energy dissipated on the electron collector and therefore its temperature and stress amplitudes. From this point of view it would be very desirable to keep the ionization efficiency high.

Another important parameter is the maximum perveance of the electron beam in the central region, which is a measure of the electron-beam linear charge density, because it determines the ultimate achievable capacity of the ion trap. Electron-beam perveance in the trap region is individual for each ion source and is determined by the ratio of the electron beam and central drift tubes radii, and by the quality of the electron beam and electron optics as well. Also it is very desirable to have the perveance of the electron beam in the electron collector as high as possible considering the high electron-beam power dissipated on its walls.

Since the BNL EBIS is intended to be used as an ion source for the relativistic heavy ion collider (RHIC) facility such parameters of the ion beam as transverse and longitudinal energy spreads are important for ion-beam transmission and acceleration since they affect the chromatic aberrations and the emittance of the ion beam. For “classical” high electron current EBIS with potential well inside the drift tube

comparable to the full electron energy, these components of ion-beam energy must be properly addressed.

II. MAXIMUM PERVEANCES OF THE ELECTRON BEAM

A. Maximum perveance of the electron beam in an ion trap region

Generally one can calculate the capacity of the ion trap the using simple formula

$$Q = 3.33 \times 10^{11} \times \frac{I_{el} \times l}{\sqrt{E_{el}}},$$

where Q is the number of electrons within the ion trap, I_{el} the electron current (amperes), l the length of the ion trap (meters), and E_{el} the electron energy (keV).

For scaling the intensity of EBIS as a function of the maximum electron current $I_{el,max}$ it can be useful to exploit a concept of maximum perveance of the electron beam in a trap region P_{max} , which is a fixed parameter for this area,

$$P_{max} = \frac{I_{el,max}}{U^{1.5}},$$

where $I_{el,max}$ is the maximum achievable current for a given U (A) and U is the potential difference between the cathode of the electron gun and the trap drift tube (volts). In this case the capacity of the ion trap can be presented as

$$Q_{max} = 1.05 \times 10^{13} \times (P_{max})^{1/3} \times l \times (I_{el,max})^{2/3}.$$

Since there is a difference between the electron energy and U by the amount of potential drop in a drift tube one needs to keep in mind that this formula assumes the case of full neutralization of the electron beam by ions, when electron energy is equal to the potential difference between cathode and central drift tube.

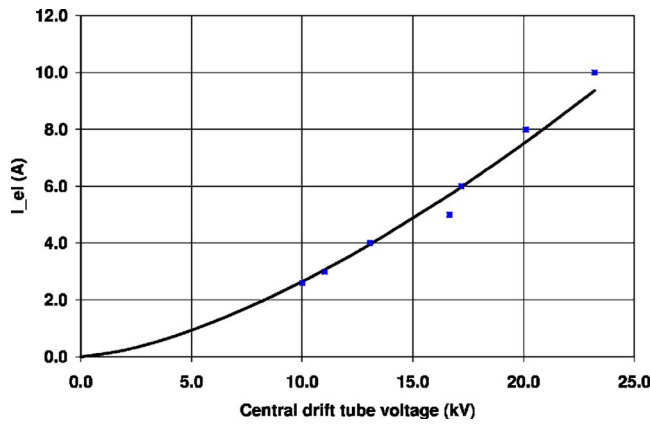


FIG. 1. Maximum perveance of the electron beam in the ion trap region of BNL Test EBIS for not neutralized electron beam. The solid line is a best fit of experimental data with perveance of $2.65 \times 10^{-6} \text{ A/V}^{1.5}$.

The goal of this set of experiments was to find a maximum electron current $I_{el,max}$ for a given voltage on a central drift tube U with respect to the cathode. The maximum electron current $I_{el,max}$ corresponds to the situation when the electron beam can still be propagated in a stable mode but a small increase of it results in a steep increase of the electron-beam loss due to formation of the virtual cathode. In this set of experiments the length of the electron pulse was ~ 1 ms and the ion trap was not neutralized. The inner diameter of the central drift tubes is 31 mm, the magnetic field on the cathode was $B_{cath}=0.14$ T, magnetic field in the trap was $B_{trap}=4.6$ T, and the cathode diameter is $d_{cath}=9.2$ mm. Figure 1 presents the measured dependence of the maximum electron current on trap drift tube voltage with respect to the cathode of the electron gun.

A good fit for our experimental data gives a current/voltage dependence of $I_{el,max}=2.65 \times 10^{-6} \times U^{1.5}$ with a not neutralized electron space charge. Since with neutralization of electrons by ions the potential difference between axis and the drift tube wall decreases one can expect higher effective perveance for the EBIS trap region.

B. Maximum perveance of the electron collector

In experiments with maximum perveance of the electron collector the goal was to find the minimum voltage on the electron collector with respect to the cathode of the electron gun for a given electron current with short electron-beam pulses (~ 1 ms). The minimum collector voltage is defined as the voltage with electron beam propagating into the electron collector but a small increase of it crashes the beam by a virtual cathode formation. No special attention to the performance of ion trap was paid since only short electron-beam pulses were used. For an electron current of $I_{el}=6.0$ A the minimum collector voltage was 4.8 kV, which corresponds to the perveance of the electron beam in the collector region $P_{col}=18 \times 10^{-6} \text{ A/V}^{1.5}$. This number is very close to a simulated maximum perveance of this electron collector ($19 \times 10^{-6} \text{ A/V}^{1.5}$). The design of RHIC EBIS electron collector is based on a much more conservative assumption of the perveance of the electron collector ($P=11 \times 10^{-6} \text{ A/V}^{1.5}$), which gives us a comfortable safety margin.

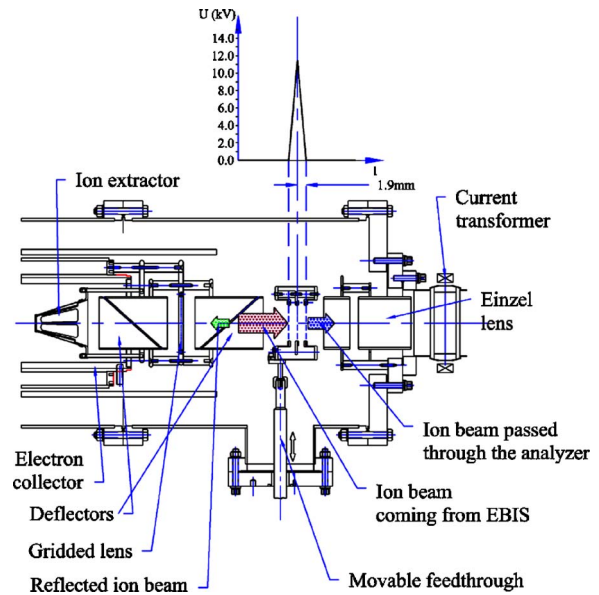


FIG. 2. Schematic of longitudinal energy spectra measurement setup.

III. ION-BEAM ENERGY SPREAD

To measure the longitudinal energy spread of the extracted ion beam a simple energy analyzer with three parallel meshes was used. The central (analyzing) mesh is isolated and the front and back meshes are grounded. The optical effect of this system on the incoming and outgoing ion beams with the voltage of the central mesh below the stopping potential proved to be negligible. This analyzer is mounted on a movable feedthrough and can be easily inserted in a beam path or retracted (Fig. 2). The same device was also used as an ion-beam chopper for an in-line time-of-flight spectrometer.

The component of full ion current, which passed the analyzer, was measured with a current transformer. In this set of experiments two values of the electron-beam current were used: 3.3 and 6.6 A. To avoid primary ion loss on an analyzer a continuous gas injection of Xe was used. Typical conditions for this experiment were confinement time $\tau_{conf}=9$ ms with the most populated Xe charge state 19+ and typical extracted total ion charge for 6.6 A was ~ 30 nC without an analyzer inserted and ~ 20 nC with an analyzer. The ion intensity for electron current $I_{el}=3.3$ A was approximately half of this value.

The experimental normalized stopping curves for a set of extraction times are presented in Fig. 3.

It is expected that the rate of ion extraction affects longitudinal energy spread, adding the energy originated from passing a rising axial potential during extraction to the internal ion temperature. A simple analytical model was developed to calculate the extraction time and the energy gain (ΔE_{grad}) of ion Au^{32+} moving a maximum distance in the trap with linear gradient, which increases linearly with time from 0 to 2 kV. Ion energy spectra for different extraction rates have been measured. An experimental value of equilibrium ion temperature 1.4 keV q was used to calculate ion energy spread $E_{calc}=1.4+\Delta E_{grad}$. Compiled experimental data on de-

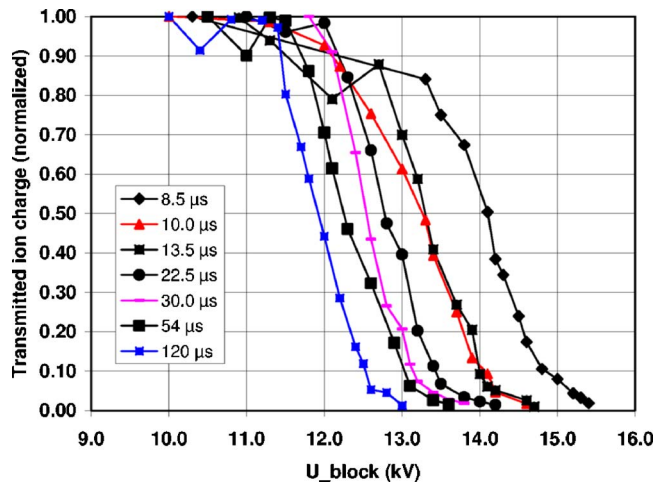


FIG. 3. Dependence of the transmitted normalized ion charge through the energy analyzer on the stopping potential for electron-beam current $I_{el} = 6.6$ A and for over-barrier extraction.

pendence of the longitudinal energy spread on the extraction time and calculated values with the above-mentioned model are presented in Fig. 4.

With slow extraction rate ($t_{extr} > 40 \mu s$) the contribution to the axial energy from the acceleration on an axial potential slope becomes very low and the axial energy at slow extraction can be interpreted as an internal ion temperature in the ion trap. For the conditions used here this temperature is $T_{ion} = 1.4 \text{ keV } q$. Information on ion temperature is essential for ongoing simulations of ion-beam extraction and transmission in low energy beam transport (LEBT) and radio frequency quadrupole (RFQ).

For the same electron current $I_{el} = 6.6$ A, longitudinal energy spectra were taken for two methods of ion extraction: by dropping the extraction potential barrier and by raising the bottom of the longitudinal potential well (Fig. 5).

With drop-the-barrier ion extraction the potential of the central drift tubes does not change and the ions are extracted during dropping the potential on the extraction barrier. With over-barrier extraction one does not change the potential of the extraction barrier and the ions are extracted by raising the potential of the central drift tubes (containing the ion trap) higher than the potential of the extraction barrier (but lower

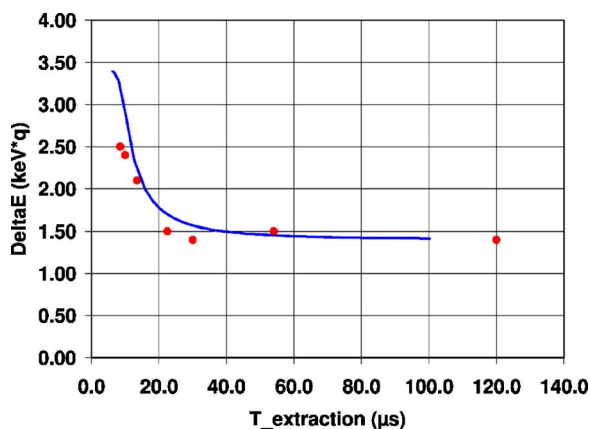


FIG. 4. Dependence of the longitudinal energy spread on the extraction time. $I_{el} = 6.6$ A. Solid line: analytical calculation.

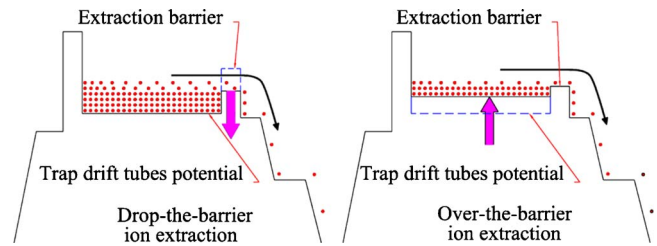


FIG. 5. Illustration of two methods of ion extraction from EBIS used in experiments.

than the potential on the opposite barrier). No additional axial gradient in these experiments was applied. The stopping curves for both methods are presented in Fig. 6.

One can see that the energy spread for ion extraction by dropping the barrier is larger than for ion extraction over the barrier. The reason for the larger energy spread for drop-the-barrier method can be an overlap of the internal ion temperature with a potential difference within the radial potential well occupied by ions, which results in different starting potentials for ions. This overlap does not happen for the over-the-barrier method because in a process of raising the bottom of the axial potential well only ions with thermal energy can come over the fixed potential of the extraction barrier.

An illustration of the longitudinal energy spread dependence on the electron-beam current and corresponding ion intensity is presented in Fig. 7 (ion intensity is not normalized).

The larger energy spread for higher electron current is caused by larger value of the radial potential well occupied by ions. It takes longer time for the same rate of the extraction ramp to cross this potential difference within radial area occupied by ions and it has larger final potential difference reflected in energy spread.

IV. EFFICIENCY OF IONIZATION

Efficiency of ionization (K) is defined here as a ratio of the calculated value of ionization factor $j\tau$ (product of electron current density in the ionization region j and ion confinement time τ) needed to produce the specific ion with the required charge state as a most populated line in a charge-

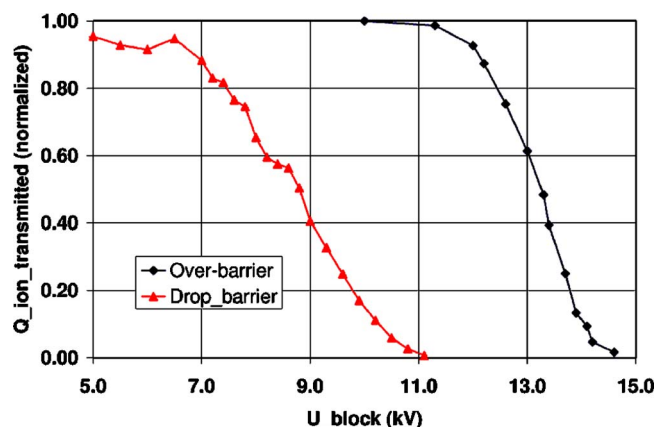


FIG. 6. Dependences of the transmitted normalized ion charge through the energy analyzer on the stopping potential for over-barrier and drop-the-barrier extraction methods ($I_{el} = 6.6$ A).

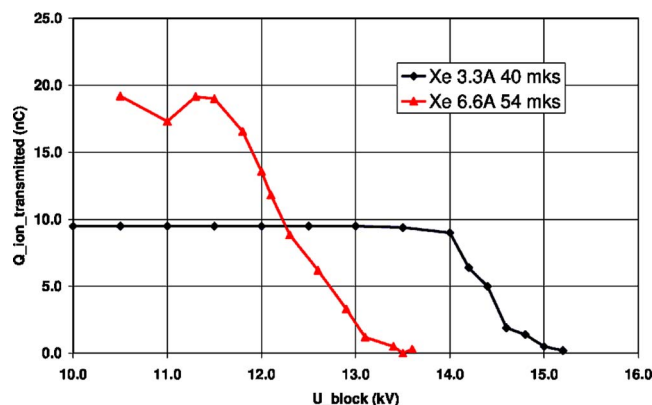


FIG. 7. Dependence of the transmitted ion charge through the energy analyzer on the stopping potential for over-barrier extraction for electron currents 3.3 and 6.6 A.

state spectrum to the experimental value of $j\tau$, which provides the same spectrum. The efficiency of ionization can also be interpreted as the fraction of time the ions spend inside the electron beam during their confinement in a potential trap.

EBIS parameters for this experiment were an electron-beam current of $I_{e1}=6.8$ A, and electron energy in an ion trap $E_{e1}=20$ keV. The calculated value of electron current density in an ion trap $j=360$ A/cm² (based on a ratio of magnetic fields on a cathode and in the ion trap for magnetically confined electron beam).

To measure the charge-state spectrum a Mamyrin-type time-of-flight (TOF) mass-spectrometer modified for better ion transmission was used. A hollow cathode ion source with Wien filter was used for injection of low-charged Au ions into EBIS trap. Au charge-state spectra were calculated with program SUK (Ref. 4) from Becker and the calculated values of ionization factor $j\tau$ are presented in Fig. 8 together with those experimentally measured from TOF spectra. The efficiency of ionization K is also shown on this figure.

This graph demonstrates that the calculated and experimentally observed spectra of Au ions are in a good agreement for any given factor $j\tau$ and therefore the EBIS ionization efficiency is close to 1 for the range of $j\tau$ needed for producing Au³²⁺ ions. One would expect the ionization efficiency to decrease at longer confinement times, due to the ion heating.

V. DISCUSSION

The results of this experimental study demonstrate that substantial increase in ion-beam intensity from a multiamperere EBIS comes with increase in ion energy spread. This increase is caused by both the internal ion temperature in the

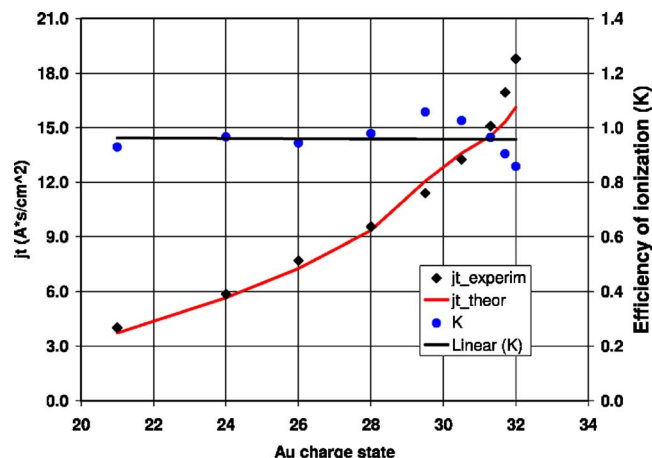


FIG. 8. Dependence of the most populated Au charge state in experimentally measured and calculated spectra on the ionization factor $j\tau$ and the ionization efficiency K .

trap and by additional energy in the axial potential gradient within the ion trap during extraction. These parameters are scalable and therefore predictable. Preliminary simulations of ion-beam extraction and transmission in the Low-Energy Beam Line (LEBT) were conducted with our experimental data on energy spread. These simulations indicate that ion-beam longitudinal energy spread and emittance even for ion pulse width as short as 10 μ s are acceptable for the RFQ accelerator.

Experimental data on the efficiency of ionization confirm that during confinement, ions spend most of the time within the electron-beam boundary.

Maximum perveance measurements agree with optical simulations for both the trap region and the electron collector. Retarding the electron beam during or after neutralization by ions in the trap allows one to increase the electron density in the trap and therefore increase the capacity of the ion trap.

Finally, these experiments demonstrate, that the high current BNL test EBIS operates as a “classical” EBIS and all of its major parameters can be calculated using simple classical EBIS phenomenological model.

ACKNOWLEDGMENT

This work was performed under the auspices of the U.S. Department of Energy.

¹E. D. Donets, Phys. Scr., T **T3**, 11 (1983).

²E. N. Beebe, J. G. Alessi, O. Gould, D. Graham, A. Kponou, A. Pikin, K. Prelec, and J. Ritter, Rev. Sci. Instrum. **73**, 699 (2002).

³A. Pikin, J. Alessi, E. Beebe, A. Kponou, and K. Prelec, Rev. Sci. Instrum. **73**, 670 (2002).

⁴R. Becker (private communication).